AMERICAN SOCIETY FOR MICROBIOLOGY | Applied and Environmental Microbiology

Metabolism of *myo*-Inositol by *Legionella pneumophila* Promotes Infection of Amoebae and Macrophages

Christian Manske,[a] Ursula Schell,[a] Hubert Hilbi[a,b]

Max von Pettenkofer Institute, Ludwig Maximilians University, Munich, Germany[a]; Institute of Medical Microbiology, University of Zürich, Zürich, Switzerland[b]

ABSTRACT

***Legionella pneumophila* is a natural parasite of environmental amoebae and the causative agent of a severe pneumonia termed Legionnaires' disease. The facultative intracellular pathogen employs a bipartite metabolism, where the amino acid serine serves as the major energy supply, while glycerol and glucose are mainly utilized for anabolic processes. The *L. pneumophila* genome harbors the cluster *lpg1653* to *lpg1649* putatively involved in the metabolism of the abundant carbohydrate *myo*-inositol (here termed inositol). To assess inositol metabolism by *L. pneumophila*, we constructed defined mutant strains lacking *lpg1653* or *lpg1652*, which are predicted to encode the inositol transporter IolT or the inositol-2-dehydrogenase IolG, respectively. The mutant strains were not impaired for growth in complex or defined minimal media, and inositol did not promote extracellular growth. However, upon coinfection of *Acanthamoeba castellanii*, the mutants were outcompeted by the parental strain, indicating that the intracellular inositol metabolism confers a fitness advantage to the pathogen. Indeed, inositol added to *L. pneumophila*-infected amoebae or macrophages promoted intracellular growth of the parental strain, but not of the Δ*iolT* or Δ*iolG* mutant, and growth stimulation by inositol was restored by complementation of the mutant strains. The expression of the P_{iol} promoter and bacterial uptake of inositol required the alternative sigma factor RpoS, a key virulence regulator of *L. pneumophila*. Finally, the parental strain and Δ*iolG* mutant bacteria but not the Δ*iolT* mutant strain accumulated [U-$^{14}C_6$]inositol, indicating that IolT indeed functions as an inositol transporter. Taken together, intracellular *L. pneumophila* metabolizes inositol through the *iol* gene products, thus promoting the growth and virulence of the pathogen.**

IMPORTANCE

The environmental bacterium *Legionella pneumophila* is the causative agent of a severe pneumonia termed Legionnaires' disease. The opportunistic pathogen replicates in protozoan and mammalian phagocytes in a unique vacuole. Amino acids are thought to represent the prime source of carbon and energy for *L. pneumophila*. However, genome, transcriptome, and proteome studies indicate that the pathogen not only utilizes amino acids as carbon sources but possesses broader metabolic capacities. In this study, we analyzed the metabolism of inositol by extra- and intracellularly growing *L. pneumophila*. By using genetic, biochemical, and cell biological approaches, we found that *L. pneumophila* accumulates and metabolizes inositol through the *iol* gene products, thus promoting the intracellular growth, virulence, and fitness of the pathogen. Our study significantly contributes to an understanding of the intracellular niche of a human pathogen.

Legionella pneumophila is a Gram-negative ubiquitous environmental bacterium that survives in complex multispecies biofilms in natural or manmade water sources (1–3). Predominantly, however, *Legionella* spp. parasitize free-living protozoa and grow within these unicellular bacterivores (4, 5). When bacteria-laden aerosols are inhaled, *L. pneumophila* reaches the lung, where the opportunistic pathogen infects and replicates within alveolar macrophages (6). Growth in amoebae evolutionarily predates and appears to mechanistically mirror growth in macrophages, which is a prerequisite to causing a fulminant pneumonia termed Legionnaires' disease (6).

The key virulence factor governing the intracellular replication of *L. pneumophila* is the Icm/Dot type IV secretion system (T4SS), composed of 25 *icm* or *dot* gene products, most of which are functionally essential. This T4SS delivers into the host cell more than 300 different "effector proteins," many of which target and subvert central cell processes to create a replication-permissive endoplasmic reticulum (ER)-derived *Legionella*-containing vacuole (LCV) (7–10). Hence, a *L. pneumophila* strain lacking, e.g., *icmT*, does not form a replication-permissive LCV and is defective for intracellular growth. A crucial regulatory element of *L. pneumophila* intracellular growth is RpoS. The alternative sigma factor controls the switch from the replicative avirulent phase to the stationary virulent phase of *L. pneumophila* (11–13) and also regulates the *Legionella* quorum-sensing system Lqs (14, 15).

While LCV formation is the focus of extensive ongoing studies, the intracellular metabolism of *L. pneumophila* and its implications for bacterial virulence remain a rather uncharted field (16, 17). *L. pneumophila* is an obligate aerobe that primarily relies on certain amino acids as carbon and energy sources and is auxotrophic for several other amino acids, including arginine, cysteine, isoleucine, leucine, methionine, serine, and threonine (18–21).

Received 1 April 2016 **Accepted** 6 June 2016

Accepted manuscript posted online 10 June 2016

Citation Manske C, Schell U, Hilbi H. 2016. Metabolism of *myo*-inositol by *Legionella pneumophila* promotes infection of amoebae and macrophages. Appl Environ Microbiol 82:5000–5014. doi:10.1128/AEM.01018-16.

Editor: A. M. Spormann, Stanford University

Address correspondence to Hubert Hilbi, hilbi@imm.uzh.ch.

Supplemental material for this article may be found at http://dx.doi.org/10.1128/AEM.01018-16.

Isotopologue profiling studies with stable [^{13}C] isotopes indicated that serine is a major carbon and energy source for *L. pneumophila* and readily metabolized by the bacteria (22).

The genomes of *L. pneumophila* strains revealed that the bacterium also possesses complete pathways for the metabolism of carbohydrates (23–25), and the utilization of these compounds has already been indicated in earlier studies (21, 26). More recent physiological and isotopologue profiling studies established that glucose and glycerol are metabolized by *L. pneumophila* under extracellular and intracellular conditions (22, 27, 28). *L. pneumophila* employs a bipartite metabolism, where amino acids, such as serine, are preferentially catabolized and serve as a major supplier of energy, while glycerol and carbohydrates, like glucose, are predominantly utilized for anabolic processes (28). A bipartite metabolic strategy is also employed by other intracellular pathogens, like *Listeria monocytogenes* (29) or *Mycobacterium tuberculosis* (30, 31), and might be an adaptation to an intracellular lifestyle providing the bacteria with a variety of different carbon sources.

The carbohydrate *myo*-inositol (here referred to as inositol) is commonly found in many soil and aquatic ecosystems and exists in mono- or polyphosphorylated forms (1-6 phosphate groups) (32). The most common form of phosphorylated inositol is inositol hexakisphosphate, also known as phytate or phytic acid. Phytate makes up more than 80% of the organic phosphate in soil (32), serves as a major phosphorus storage compound in plants and seeds (33, 34), and is a potent chelator of bivalent metal ion micronutrients, thus restricting their bioavailability (35). *L. pneumophila* produces the Icm/Dot T4SS-translocated phytase LppA, which appears to be implicated in detoxifying bacteriostatic phytate within amoebae (36).

A number of bacteria can extracellularly grow on inositol as a sole source of carbon and energy. These include *Bacillus subtilis* (37), *Lactobacillus casei* (38), *Salmonella enterica* (39), and *Sinorhizobium meliloti* (40). The molecular genetics of bacterial inositol catabolism have been best studied in *B. subtilis*, in which two operons, *iolABCDEFGHIJ* and *iolRS*, as well as the orphan gene *iolT*, are implicated in inositol degradation (37). IolT and IolF have been identified as inositol transporters of the major facilitator superfamily, but only mutants lacking *iolT* showed major growth defects (41). Another central component of inositol catabolism in *B. subtilis* is the regulator protein IolR, which positively regulates the expression of all *iol* genes in the presence of inositol (42).

Although the genetic organization and setup of *iol* genes can differ among organisms (Fig. 1A), the principal reactions are conserved and comprise seven steps (Fig. 1B) (37, 39). After the import of inositol by the transporter IolT, the polyol is oxidized in a first step to 2-keto-*myo*-inositol, which is catalyzed by the inositol-2-dehydrogenase IolG. Following several additional steps, including hexane ring cleavage and phosphorylation, the end products dihydroxyacetone phosphate and acetyl-coenzyme A (CoA) are channeled into the central cell metabolism.

In this study, we show that *L. pneumophila* mutant strains lacking *lpg1653* (*iolT*) or *lpg1652* (*iolG*) are outcompeted by the parental strain upon coinfection of *Acanthamoeba castellanii* and, dependent on the presence of *iolT* and *iolG*, inositol added to *L. pneumophila*-infected amoebae or macrophages promotes intracellular bacterial growth. Moreover, IolT was found to function as an inositol transporter, and expression of the P_{iol} promoter as well as bacterial uptake of inositol required the alternative sigma factor RpoS. In summary, our results indicate that intracellular inositol metabolism promotes the growth and virulence of *L. pneumophila*.

MATERIALS AND METHODS

Bacteria, cells, and growth conditions. *L. pneumophila* strains (Table 1) were cultured under aerobic conditions at 37°C in *N*-(2-acetamido)-2-aminoethanesulfonic acid (ACES)-buffered yeast extract (AYE) broth or grown on charcoal yeast extract (CYE) agar plates supplemented with chloramphenicol (Cm; 5 μg ml^{-1}) or kanamycin (Km; 50 μg ml^{-1} in broth or 10 μg ml^{-1} in agar plates), if necessary. Alternatively, *L. pneumophila* was cultivated at 37°C in chemically defined medium (CDM) (22), modified from Ristroph et al. (19), or minimal defined medium (MDM) (28). CDM and MDM were prepared by dissolving components in 950 ml of double-distilled water (ddH_2O). The pH was adjusted to 6.3 (CDM) or 6.5 (MDM) using KOH, and dissolved Fe-pyrophosphate was added and filled up to 1 liter. *Escherichia coli* TOP10 was used for cloning and grown in LB medium at 37°C containing 30 μg ml^{-1} Cm or 50 μg ml^{-1} Km, if necessary.

For extracellular growth assays, *L. pneumophila* JR32 or mutant strains were resuspended from CYE agar plates in CDM with a starting optical density at 600 nm (OD_{600}) of 0.1. To this end, 3-ml cultures were prepared in 13-ml plastic tubes (Sarstedt, Nümbrecht, Germany) for each strain in triplicate and incubated at 37°C on a turning wheel for 15 to 18 h until the cultures reached an OD_{600} of 0.5 to 0.8. The cultures were diluted to OD_{600} of 0.1 in 3 ml of CDM or MDM, and 10 mM inositol was added where indicated. The bacteria were then further incubated at 37°C on a turning wheel for 48 h, and the optical density was assessed.

Acanthamoeba castellanii (ATCC 30234, lab collection) was grown in peptone yeast glucose (PYG) medium at 23°C. *Dictyostelium discoideum* Ax3 (Zhou et al. [43], lab collection) was grown axenically in HL5 medium at 23°C. Murine RAW 264.7 macrophages (ATCC TIB-71, lab collection) were cultivated in RPMI 1640 medium (Gibco) containing 10% heat-inactivated fetal bovine serum (FBS) and 2 mM glutamine in 37°C/5% CO_2.

Construction of vectors for allelic exchange, gene expression, and green fluorescent protein reporter assays. For sequence analysis, the *Legionella* homepage of the Institut Pasteur (http://genolist.pasteur.fr/LegioList/index.html) and the NCBI database (http://www.ncbi.nlm.nih.gov/) were used. Allelic exchange vector pCM003 (Table 1) was constructed using 0.5 to 0.8 kb of 5′- and 0.5 to 0.8 kb of 3′-flanking regions of *iolT* and a Km resistance cassette, and allelic vector pCM022 was constructed using 0.5 to 0.8 kb of 5′- and 0.5 to 0.8 kb of 3′-flanking regions of *iolG* and a Km resistance cassette. For the flanking regions of *iolT*, primer pair *iolT*-LB-XbaI-fo and *iolT*-LB-SalI-re and primer pair *iolT*-RB-SalI-fo and *iolT*-RB-XbaI-re were used (see Table S1 in the supplemental material). For the flanking regions of *iolG*, primer pair *iolG*-LB-XbaI-fo and *iolG*-LB-SalI-re and primer pair *iolG*-RB-SalI-fo and *iolG*-RB-XbaI-re were used. The amplified PCR products of these flanking regions were digested using the restriction enzymes SalI and XbaI. The plasmid pUC4K was digested with SalI, yielding a 1.4-kb fragment containing the Km resistance cassette. The suicide vector pLAW344 was digested using the restriction enzyme XbaI. The corresponding flanking regions and the Km resistance cassette were cloned into pLAW344 in a four-way ligation, transformed into *E. coli* TOP10, and selected for the Km resistance cassette. The plasmids were analyzed by restriction digestion and sequenced.

For complementation of the Δ*iolT* mutant or Δ*iolG* mutant strain, the vectors pCM020 and pCM023 were constructed using the primer pair *iolT*-BamHI-fo-comp and *iolT*-SalI-re-comp or *iolG*-BamHI-fo-comp and *iolG*-SalI-re-comp. The PCR products were cloned into vector pCR033 using BamHI and SalI. For the construction of plasmid pCM004, an instable form of green fluorescent protein (GFP), GFP(ASV), was used (44). To this end, plasmid pJBA132 was digested using XbaI and HindIII, yielding a 0.75-kb fragment containing *gfp*(ASV), which was cloned into plasmid pMMB207C. The 400-bp promoter region of *iolT* was amplified using the primers *iolT*-

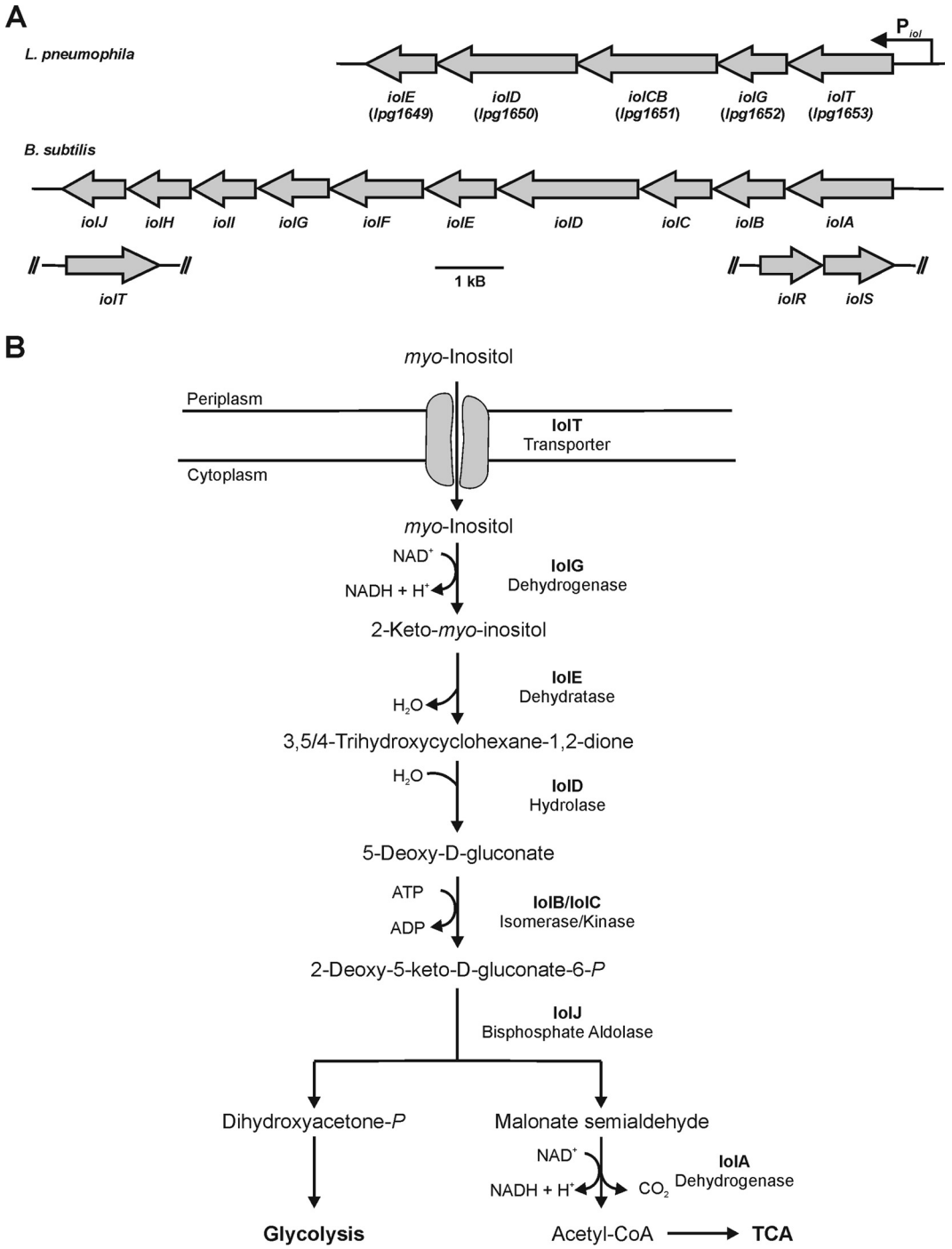

FIG 1 The *L. pneumophila iol* operon and pathway of *myo*-inositol catabolism. (A) The *L. pneumophila lpg1653* to *lpg1649* gene cluster forms the *iol* operon that contains five genes predicted to be involved in the metabolism of *myo*-inositol. The genes encode the putative inositol transporter IolT and the inositol catabolism enzymes IolG, IolCB, IolD, and IolE. The arrangement of the *B. subtilis iol* genes is shown for comparison. (B) For catabolism, inositol is taken up through the transporter IolT and oxidized to 2-keto-*myo*-inositol catalyzed by the inositol-2-dehydrogenase IolG. The dehydratase IolE produces 3,5/4-trihydroxy-cyclohexane-1,2-dione, which is linearized to 5-deoxy-gluconate catalyzed by the hydrolase IolD. IolB and IolC catalyze an isomerization and phosphorylation, yielding 2-deoxy-5-keto-D-gluconate and the central intermediate 2-deoxy-5-keto-D-gluconate-6-phosphate, respectively, which in *B. subtilis* and *S. enterica* are cleaved by the bisphosphate aldolase IolJ, yielding dihydroxyacetone phosphate and malonate semialdehyde. Malonate semialdehyde is converted into acetyl-CoA by the decarboxylating malonate-semialdehyde dehydrogenase IolA. The scheme is adapted from Yoshida et al. (37) and Kröger and Fuchs (39). TCA, tricarboxylic acid cycle.

TABLE 1 Strains and plasmids used in this study

Strain/plasmid	Relevant properties/description[a]	Reference or source
Strains		
E. coli		
TOP10		Invitrogen
L. pneumophila		
JR32	*L. pneumophila* serogroup 1 Philadelphia-1, salt-sensitive isolate of AM511	76
GS3011 (Δ*icmT* mutant)	*L. pneumophila* JR32 *icmT3011*::Km	77
CM02 (Δ*iolT* mutant)	*L. pneumophila* JR32 *lpg1653*::Km	This study
CM03 (Δ*iolG* mutant)	*L. pneumophila* JR32 *lpg1652*::Km	This study
AK01 (Δ*lqsT* mutant)	*L. pneumophila* JR32 *lqsT*::Km	47
AK02 (Δ*lqsS* Δ*lqsT* mutant)	*L. pneumophila* JR32 *lqsS*::Km *lqsT*::Gm	47
NT02 (Δ*lqsA* mutant)	*L. pneumophila* JR32 *lqsA*::Km	56
NT03 (Δ*lqsR* mutant)	*L. pneumophila* JR32 *lqsR*::Km	14
NT05 (Δ*lqsS* mutant)	*L. pneumophila* JR32 *lqsS*::Km	56
LM1376 (Δ*rpoS* mutant)	*L. pneumophila* JR32 *rpoS4*::Tn*903*dIIGm	12
Plasmids		
pCM003	pLAW344, *iolT*::Km	This study
pCM004	pMMB207C-*gfp*(ASV)	This study
pCM007	pMMB207C-P_{iol}-*gfp*(ASV)	This study
pCM020	pCR033-M45-*iolT*	This study
pCM022	pLAW344, *iolG*::Km	This study
pCM023	pCR033-M45-*iolG*	This study
pCR033	*Legionella* expression vector, Δ*mobA*, RBS, M45-(Gly)5, Cm (=pMMB207C-RBS-M45)	48
pJBA132	pUC18-*luxR*-P_{luxI}-RBS-*gfp*(ASV)	78
pLAW344	*oriT* (RK2), *oriR* (ColE1), *sacB*, Cm, Ap	45
pMMB207C	Expression vector, Δ*mobA*, RBS, Cm	48
pNT028	pMMB207C, *gfp* (constitutive)	14
pSW001	pMMB207C-RBS-*dsred* (constitutive)	3
pUC4K	*oriR* (pBR322), Ap, MCS::Km	Amersham

[a] Km, kanamycin resistance; Gm, gentamicin resistance; RBS, ribosome binding site; Cm, chloramphenicol resistance; Ap, ampicillin resistance.

400bp-SacI-fo and *iolT*-400bp-XbaI-re. The PCR product was cloned into pCM004 using SacI/XbaI, yielding plasmid pCM007.

Construction of chromosomal deletion mutant strains. To generate the deletion mutant strains CM02 (Δ*iolT*) or CM03 (Δ*iolG*), *iolT* or *iolG* was deleted in the chromosome of *L. pneumophila* JR32, as described previously (14, 45). To this end, strain JR32 was transformed with pCM003 or pCM022 by electroporation and plated on CYE agar plates containing 10 μg ml^{-1} Km. The plates were incubated at 30°C for 5 days, and kanamycin-resistant (Km^r) colonies were selected and grown overnight in 96-well plates in AYE broth with 50 μg ml^{-1} Km. The cultures were then spotted on CYE-Km, CYE-Km–2% sucrose, and CYE-Cm plates in parallel and grown at 30°C to select for chloramphenicol-sensitive (Cm^s)/Km^r/sucrose-resistant (Suc^r) colonies. Double-crossover mutants were confirmed by PCR and sequenced.

Intracellular replication of *L. pneumophila*. Intracellular replication of *L. pneumophila* was assessed as previously published (46). In brief, *A. castellanii* or *D. discoideum* amoebae were grown in PYG or HL5 medium, respectively, to ~80% confluence, and 4×10^4 cells per well were seeded in 96-well plates. The plates were incubated overnight at 23°C to allow replication of the amoebae. PYG or HL5 medium was exchanged with LoFlo medium (ForMedium). *L. pneumophila* strains harboring plasmid pNT28 (constitutive GFP production) were grown in AYE-Cm (5 μg ml^{-1}) to an OD_{600} of 3 and used to infect the amoebae (multiplicity of infection [MOI], 10 to 20). Infections were synchronized by centrifugation at 500 × *g* for 10 min, and the plates were incubated at 30°C. A concentration of 10 to 20 mM inositol was added either concurrently with infection or 2 h or 4 h postinfection to some wells, and GFP fluorescence was measured in a plate spectrophotometer at specific intervals.

For determining CFU, *A. castellanii* or RAW 264.7 macrophages were seeded at 5×10^4 cells per well into 96-well plates. To this end, the cells were suspended in Ac buffer [4 mM $MgSO_4 \cdot 7H_2O$, 0.4 mM $CaCl_2$, 3.4 mM sodium citrate dihydrate, 0.05 mM $Fe(NH_4)_2(SO_4)_2 \cdot 6H_2O$, 0.05 mM $Na_2HPO_4 \cdot 7H_2O$, 2.5 mM KH_2PO_4, 0.05 mM NH_4Cl (pH 6.5)] or RPMI 1640 medium, respectively, and the plates were incubated at 23°C (amoebae) or 37°C/5% CO_2 (macrophages) for 1 h to allow adhesion of the cells. *L. pneumophila* was grown for 21 h in AYE, as outlined above. For complementation experiments, the Δ*iolT* mutant or Δ*iolG* mutant strain producing plasmid-borne *iolT* (pCM020) or *iolG* (pCM023) under the control of the P_{tac} promoter was cultured with 1 mM isopropyl-β-D-thiogalactopyranoside (IPTG). The phagocytes were infected with *L. pneumophila* (MOI, 0.1) by centrifugation at 500 × *g* for 10 min. During the course of infection, the infected cells were then kept at 30°C (amoebae) or 37°C/5% CO_2 (macrophages), first for 1 h, and then washed with Ac buffer or RPMI 1640 medium and further incubated. Inositol at 20 mM was added 4 h postinfection to certain wells. After 48 h (macrophages) or 72 h (amoebae), cells were lysed with 0.8% saponin, and appropriate dilutions were plated on CYE agar plates to determine CFU.

***A. castellanii* competition assays.** The amoeba competition assay was performed as described previously (47). Briefly, *L. pneumophila* JR32 and mutant strains to be tested were resuspended from CYE plates in AYE broth to a starting OD_{600} of 0.1 and incubated at 37°C until the cultures reached an OD_{600} of 3. Prior to infection, 5×10^4 *A. castellanii* amoebae were seeded in a 96-well plate in Ac buffer. The plate was incubated for at least 1 h at 30°C. *A. castellanii* was then infected at a 1:1 ratio with *L. pneumophila* JR32 and the Δ*iolT* mutant or Δ*iolG* mutant strain (MOI, 0.01 each). The infection was synchronized by centrifugation at 500 × *g* for 10 min, and the plate was incubated at 37°C for 1 h. The Ac buffer was exchanged and the plate further incubated at 37°C. After 3 days, fresh amoebae were seeded into a new 96-well plate (5×10^4 cells per well in 200 μl of Ac buffer) and incubated at 30°C for 1 h. Supernatant from the old 96-well plate was harvested, and the remaining cells in the wells were lysed with 0.8% saponin. The supernatant and lysate were combined, diluted

1:1,000, and used to infect the fresh amoebae (50 μl per well). Aliquots of combined supernatant and lysate were plated in parallel on CYE agar plates and on plates containing Km (10 μg ml^{-1}) to determine CFU and to distinguish between JR32 and Km-resistant mutant bacteria. The freshly infected 96-well plate was further incubated at 37°C for another 3 days, and then lysis and reinfection were repeated.

Uptake of 2-NBDG and (immuno)fluorescence experiments. A total of 2.5×10^5 *D. discoideum* cells in 0.5 ml of HL5 medium were seeded onto poly-L-lysine-coated sterile coverslips in a 24-well plate and incubated overnight at 23°C, such that around 5×10^5 cells were present on each coverslip. The amoebae were infected with *L. pneumophila* JR32, Δ*iolT* mutant, Δ*iolG* mutant, Δ*icmT* mutant, or Δ*rpoS* mutant harboring plasmid pSW001 (constitutive DsRed production) at an MOI of 10. Infection was synchronized by centrifugation at 500 × *g* for 10 min. The cells were incubated for 1 h at 25°C, the supernatant was removed, and 0.5 ml of Sörensen phosphate buffer with $CaCl_2$ (SorC; 15 mM KH_2PO_4, 2 mM Na_2HPO_4, 50 μM $CaCl_2$ [pH 6.0]) was added per well. Subsequently, 20 μM 2-deoxy-2[(7-nitro-2,1,3-benzoxadiazol-4-yl)amino]-D-glucose (2-NBDG; Sigma-Aldrich), a fluorescent glucose analogue, was added, and the cells were further incubated at 25°C for 30 min. The cells were washed with SorC, and coverslips were then mounted on glass slides using Vectashield mounting medium (Vector Laboratories) supplemented with 1 μg ml^{-1} DAPI (4′,6-diamidino-2-phenylindole) to stain DNA. The samples were analyzed using a Leica TCS SP5 confocal microscope (HCX PLAPO CS, objective 63×/1.4 to 0.60 oil).

To homogenize infected cells for immunofluorescence microscopy, 8.5×10^5 *D. discoideum* amoebae per well were seeded in a 6-well plate, grown overnight, and infected with *L. pneumophila* (MOI, 10; 3 wells per strain). Infection was performed at 25°C for 1 h, cells were washed with SorC, and 20 μM 2-NBDG was added. The amoebae were further incubated for 30 min at 25°C, washed with SorC, suspended in homogenization buffer (20 mM HEPES, 250 mM sucrose, 0.5 mM EGTA [pH 7.2]), and lysed by nine passages through a cell homogenizer (exclusion size, 8 μm; Isobiotec) kept on ice. The homogenate was centrifuged onto poly-L-lysine-coated coverslips, followed by an antibody stain against the LCV-bound *L. pneumophila* effector SidC (48). To this end, coverslips were incubated with blocking solution (5% FBS in SorC) for 1 h and incubated with 30 μl of affinity-purified anti-SidC antiserum (diluted 1:100 in blocking solution) for 1 h at room temperature. The coverslips were washed three times with SorC, and 30 μl of appropriate secondary antibodies (diluted 1:200 in blocking solution) coupled to DyLight650 (donkey anti-rabbit IgG; Abcam) or rhodamine (bovine anti-rabbit IgG; Santa Cruz) was added and incubated for 30 min. The coverslips were washed with SorC and mounted onto glass slides using Vectashield.

Transport of [^{14}C]inositol by *L. pneumophila*. *L. pneumophila* JR32, the Δ*iolT* mutant, or the Δ*iolG* mutant was grown in AYE broth to an OD_{600} of 2.8. For complementation of the Δ*iolT* mutant, the mutant strain, harboring plasmid pCM020, was grown in AYE-Cm broth with 1 mM IPTG to allow the expression of *iolT*. The cultures were supplemented with 10 mM inositol spiked with 1% of a 1:10 dilution of [U-$^{14}C_6$]inositol (specific activity, 300 mCi/mmol; American Radiolabeled Chemicals). The bacteria were further incubated at 37°C with gentle shaking, and 200-μl samples were taken after 0, 10, 20, 30, 60, and 90 min. The samples were filtered through cellulose acetate filter disks (pore size, 0.25 μm; Roth), and filters were washed three times with phosphate-buffered saline (PBS). Filter-associated radioactivity was determined in a liquid scintillation counter (1450 MicroBeta TriLux; PerkinElmer) with EcoLume scintillation cocktail (MP Biomedicals). In another experimental setup, *L. pneumophila* JR32 or the Δ*rpoS* mutant was grown in AYE broth. Two-hundred-microliter samples were taken at OD_{600} of 0.5, 1.0, 2.0, and 3.0. Cells were incubated with 10 mM inositol spiked with 1% of a 1:10 dilution of [U-$^{14}C_6$]inositol for 20 min, filtered, washed, and measured as described above.

For determining protein-associated radioactivity, *L. pneumophila* JR32, the Δ*iolT* mutant, or the Δ*iolG* mutant was grown in AYE broth to an OD_{600} of 2.0. Cultures were supplemented with 10 mM inositol spiked with 1% of a 1:10 dilution of [U-$^{14}C_6$]inositol and further incubated at 37°C with gentle shaking. Two-hundred-microliter samples were taken after 0, 2, 4, 6, and 8 h, mixed with 1 ml of 50% trichloroacetic acid, and incubated on ice for 1 h. Samples were filtered through cellulose nitrate filter disks (pore size, 0.45 μm; Roth), and filters were washed three times with PBS. Filter-associated radioactivity was determined in a liquid scintillation counter with EcoLume scintillation cocktail.

GFP reporter assays. *L. pneumophila* JR32, the Δ*rpoS* mutant, or different *lqs* mutant strains harboring plasmid pCM007 was grown overnight in AYE-Cm broth to an OD_{600} of 1.5 to 2.0. The bacteria were diluted in AYE-Cm broth to an initial OD_{600} of 0.1 in a black 96-well clear-bottom plate (PerkinElmer), and 10 mM inositol or 6 mM serine was added to some wells. The plate was incubated in a shaking incubator at 37°C and 600 rpm for 24 h. Every hour, the optical density and GFP fluorescence were measured using a plate spectrophotometer (Optima FLUOstar; BMG Labtech).

RESULTS

A putative inositol degradation cluster in the genome of *L. pneumophila*. The genome of *L. pneumophila* harbors a group of genes putatively involved in inositol metabolism (Fig. 1). The gene cluster comprises a 7-kb region on the chromosome of *L. pneumophila* strain Philadelphia-1 and contains five genes, *lpg1653* to *lpg1649*. The genes are organized in an operon, as predicted by the Database for prOkaryotic OpeRons (DOOR^2) (http://csbl.bmb.uga.edu/DOOR/) (49) and the prokaryotic operon database (http://operons.ibt.unam.mx/OperonPredictor/), with a predicted promoter termed P_{iol} in the 400-bp region between the genes *lpg1653* and *lpg1654*. The transcriptional start site and operon organization (operon 326) have been experimentally verified by RNA deep sequencing (50). The operon is conserved in several *L. pneumophila* strains, including Philadelphia-1 (*lpg1653* to *lpg1649*), Paris (*lpp1624* to *lpp1620*), and Lens, Corby, and Alcoy (23–25), as well as in *Legionella longbeachae* (51, 52).

The proteins encoded in this operon are annotated as IolG (Lpg1652), a *myo*-inositol-2-dehydrogenase; IolCB (Lpg1651), a combined 5-dehydro-2-deoxygluconokinase–5-deoxy-glucuronate isomerase protein; IolD (Lpg1650), an inositol catabolism hydrolase protein; and IolE (Lpg1649), an inosose dehydratase (Fig. 1). These proteins show sequence identities between 30% and 50% with the corresponding proteins of *B. subtilis* and *S. enterica*. The first gene in the *lpg1653* to *lpg1649* operon is annotated as that encoding a D-xylose proton symporter and shares 32% and 30% identity with the genes encoding the inositol transporter protein IolT of *B. subtilis* and *S. enterica*, respectively. The inositol metabolism enzymes apparently missing in *L. pneumophila* are the bisphosphate aldolase IolJ and the malonate-semialdehyde dehydrogenase IolA. Moreover, no homologue of the major regulator protein IolR seems to be encoded in the genome of *L. pneumophila*, and thus, the *iol* operon is likely differently regulated compared to *B. subtilis* (37) or *S. enterica* (39).

***L. pneumophila* lacking *iolT* or *iolG* is outcompeted by the parental strain in amoebae.** To assess the role of the putative inositol degradation *iol* gene cluster for inositol metabolism and virulence of *L. pneumophila*, the mutant strains CM02 and CM03 lacking *lpg1653* (*iolT*, the putative inositol transporter) or lacking *lpg1652* (*iolG*, the inositol-2-dehydrogenase) were constructed (Table 1). The growth of these mutants was monitored in different media in the presence or absence of inositol. The parental *L. pneumophila* strain, the Δ*iolT* mutant, and the Δ*iolG* mutant strain

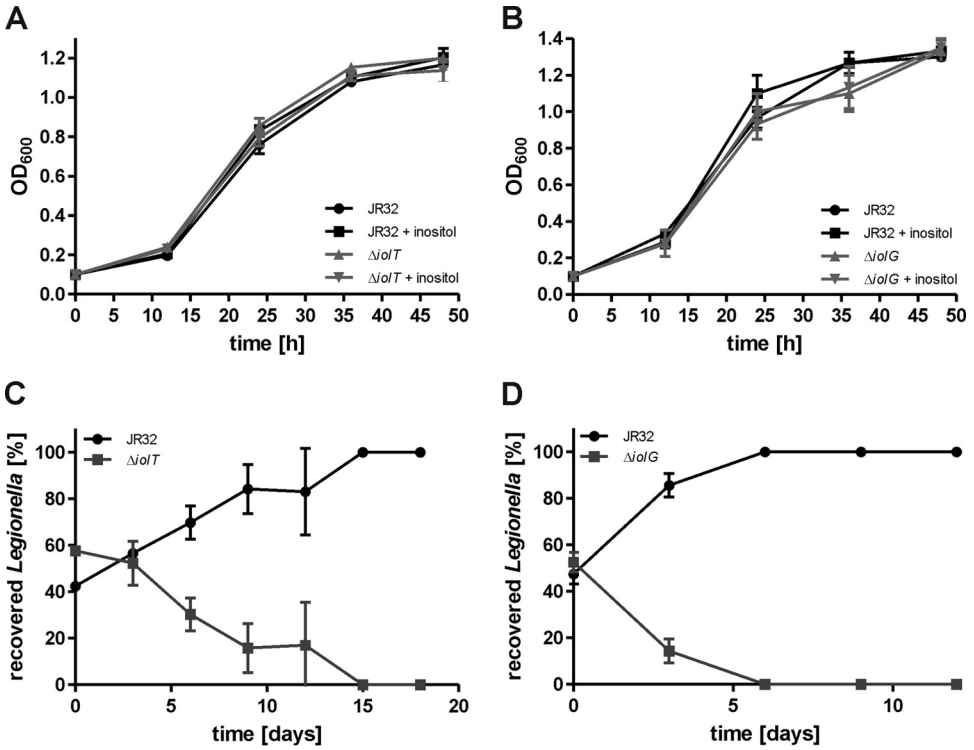

FIG 2 *L. pneumophila* lacking *iolT* or *iolG* is outcompeted by the parental strain in amoebae. Extracellular growth of *L. pneumophila* JR32 and mutant strains lacking (A) *iolT* (Δ*iolT*, *lpg1653*) or (B) *iolG* (Δ*iolG*, *lpg1652*) in MDM with and without 10 mM inositol was assessed by optical density at 600 nm (OD_{600}) at the time points indicated. For amoeba competition assays, *A. castellanii* was infected at a 1:1 ratio (MOI, 0.01 each) with *L. pneumophila* JR32 and the Δ*iolT* mutant (C) or JR32 and the Δ*iolG* mutant (D). The amoebae were lysed 3 days postinfection, and the homogenate was used to infect fresh amoebae. Bacterial numbers were determined by CFU. Mean and standard deviation (SD) of triplicates are shown (Student's *t* test; C, >6 days, $P < 0.05$; D, >3 days, $P < 0.01$). The data are representative of the results from three independent experiments.

grew indistinguishably in AYE broth (data not shown), CDM minimal medium (see Fig. S1 in the supplemental material), and MDM minimal medium (Fig. 2A and B), and the addition of 10 mM inositol did not alter the growth of strains in any medium tested.

We then analyzed whether the *iol* genes affect the interactions of *L. pneumophila* with *A. castellanii* by using the amoeba competition assay (47). Upon coinfection of *A. castellanii* at a 1:1 ratio with the parental strain and the Δ*iolT* mutant (Fig. 2C) or Δ*iolG* mutant (Fig. 2D), the mutant strains were outcompeted by the parental strain within 15 or 6 days, respectively. Hence, the Δ*iolG* mutant strain appears to have an even stronger phenotype than the Δ*iolT* mutant in the amoeba competition assay. These results indicate that *iolT* and *iolG* have a nonredundant function for *L. pneumophila*-amoeba interactions and suggest that inositol metabolism confers a fitness advantage to the pathogen.

Inositol promotes intracellular growth of *L. pneumophila* dependent on *iolT* or *iolG*. The expression of genes of the *iol* cluster is upregulated upon intracellular growth of *L. pneumophila* in human macrophages (53), suggesting that inositol plays a role during the intracellular growth of *L. pneumophila*. To assess the impact of inositol on the intracellular growth of *L. pneumophila* in amoebae, we used GFP fluorescence or CFU as the readout.

The addition of 20 mM inositol to *L. pneumophila*-infected *A. castellanii* cells concurrently with infection (Fig. 3A), 2 h postinfection (Fig. 3B), or 4 h postinfection (see Fig. S2 in the supplemental material) promoted intracellular bacterial growth, as judged by increased GFP fluorescence levels. Inositol did not increase the growth rate of exponentially growing bacteria but led to higher cell numbers beyond 24 h postinfection, suggesting that the substrate might be used only at later stages of infection. Growth promotion was dependent on *iolT*, since the addition of 20 mM inositol to *A. castellanii* infected with the Δ*iolT* mutant did not result in higher GFP fluorescence levels (Fig. 3A and B). Without the addition of inositol, the Δ*iolT* mutant grew intracellularly comparably to the parental strain under the conditions used. Finally, *L. pneumophila* Δ*icmT* lacking a functional Icm/Dot T4SS did not grow at all, i.e., GFP fluorescence did not increase throughout the experiment (data not shown).

Using CFU as a readout, the addition of 20 mM inositol to *L. pneumophila* strain JR32 growing in *A. castellanii* (Fig. 3C) or in murine macrophages (Fig. 3D) also promoted intracellular growth. Under these conditions, inositol yielded approximately 20 to 25% more CFU within 2 to 3 days of the experiment. Inositol did not affect the intracellular growth of the Δ*iolT* mutant, and the mutant strain was not impaired for intracellular growth *per se* (Fig. 3C and D).

Intracellular growth of *L. pneumophila* in the presence or absence of inositol was also tested with the Δ*iolG* mutant strain (Fig. 3E). Again, the addition of inositol to *A. castellanii* infected with strain JR32 resulted in elevated GFP fluorescence levels. However, *L. pneumophila* lacking *iolG* showed a slight intracellular growth defect, in contrast to the Δ*iolT* mutant. Hence, similar to the amoeba competition test (Fig. 2C and D), the intracellular repli-

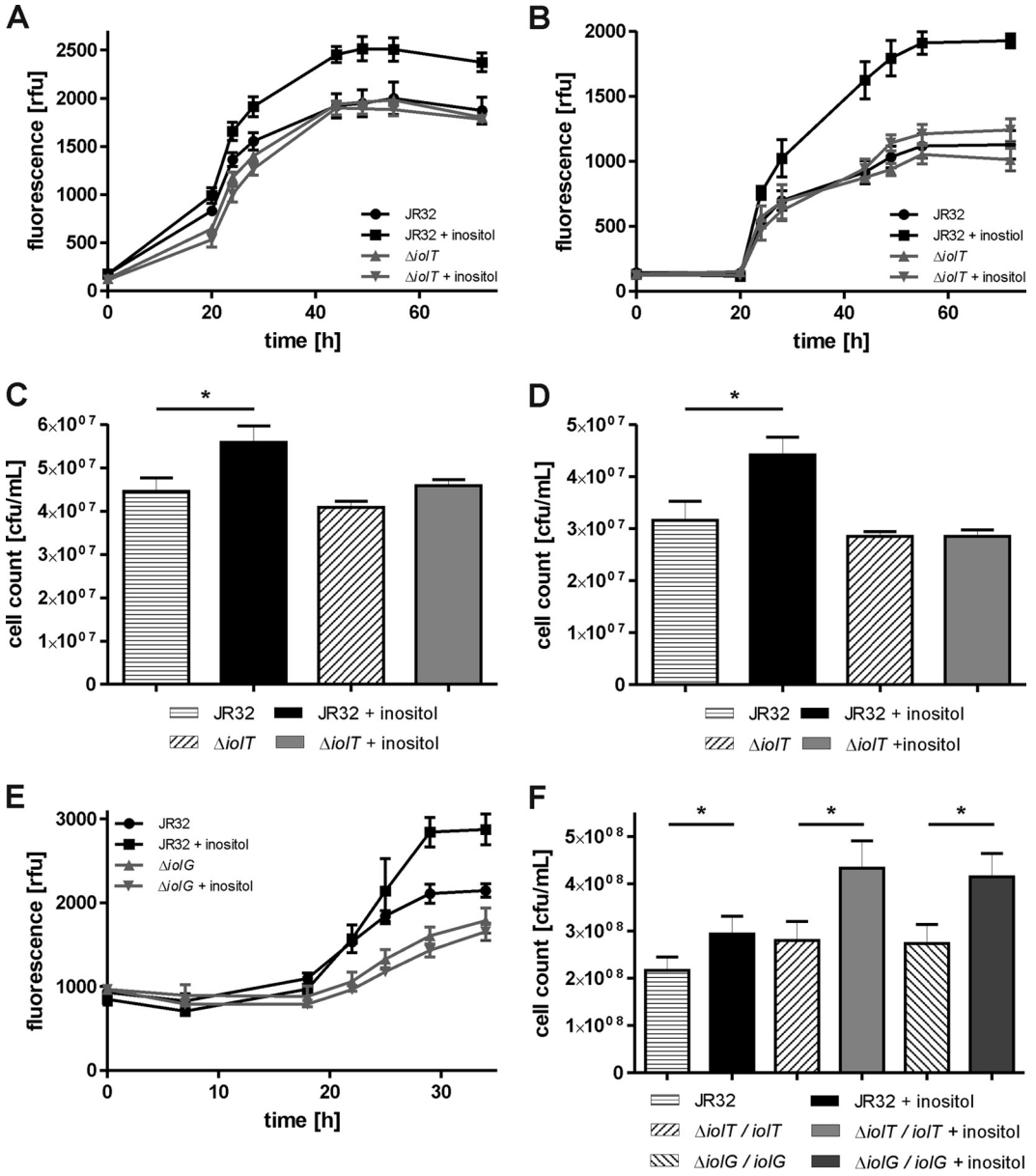

FIG 3 Inositol promotes intracellular growth of *L. pneumophila* dependent on *iolT* or *iolG*. *A. castellanii* was infected (MOI, 20) with *L. pneumophila* JR32, the Δ*iolT* mutant, or the Δ*iolG* mutant harboring plasmid pNT28 (constitutive GFP production). Inositol at 20 to 50 mM was added concomitant with infection (A) or at 2 h postinfection (B and E), and intracellular replication was determined by fluorescence. (C and F) *A. castellanii* or (D) murine RAW 264.7 macrophages were infected (MOI, 0.1) with *L. pneumophila* JR32, the Δ*iolT* mutant, or the Δ*iolG* mutant harboring no plasmid (C and D) or vector control (pCR033), *iolT* (pCM020), or *iolG* (pCM023) under the control of the P_{tac} promoter (F). Inositol at 20 mM was added 4 h postinfection, cells were lysed 3 days (C and F) or 2 days (D) postinfection, and CFU were determined by plating out appropriate dilutions on CYE agar plates. rfu, relative fluorescence units. Mean and SD of triplicates are shown (Student's *t* test; *, $P < 0.05$; A, >28 h, $P < 0.05$; B, >44 h, $P < 0.01$; E, >29 h, $P < 0.05$). The data are representative of the results from three independent experiments.

cation assay revealed a stronger phenotype for the Δ*iolG* mutant than for the Δ*iolT* mutant. Analogous to the Δ*iolT* mutant, the addition of up to 50 mM inositol to *A. castellanii* 2 h postinfection with the Δ*iolG* mutant did not result in higher GFP fluorescence levels, indicating that *iolG* is also required for growth stimulation by inositol (Fig. 3E).

Finally, we tested whether *iolT* or *iolG* complements the lack of response to inositol of the corresponding Δ*iolT* and Δ*iolG* mutant strains (Fig. 3F). Indeed, inositol significantly increased the CFU obtained for the Δ*iolT* mutant or Δ*iolG* mutant harboring plasmid-borne *iolT* or *iolG* under the control of the P_{tac} promoter. In summary, the addition of inositol to *L. pneumophila*-infected *A. castellanii* or macrophages promotes intracellular bacterial growth dependent on the *iolT* or *iolG* genes, and the lack of response of the mutant strains can be complemented by providing the corresponding gene on a plasmid. Thus, inositol is metabolized through the *iol* genes by intracellular *L. pneumophila* in protozoan and mammalian phagocytes.

Carbohydrate transport to the LCV lumen in infected amoebae. The observed stimulation of intracellular growth of *L. pneumophila* by inositol added hours after an infection might be the result of direct carbohydrate metabolism by the pathogen in the LCV, or due to an indirect effect where the host cell metabolizes inositol and then the bacteria utilize more available metabolites, such as amino acids. For direct metabolism of inositol (or any other substrate) to occur, the compound has to reach the LCV lumen after being supplied from outside an infected host cell. To test the intracellular fate of inositol, we employed the social soil amoeba *Dictyostelium discoideum*, a versatile model to assess LCV formation and intracellular replication of *L. pneumophila*. Similar to *A. castellanii* (Fig. 3B and E), the addition of 10 mM inositol to *L. pneumophila*-infected *D. discoideum* 2 h postinfection promoted intracellular growth of the parental strain JR32 but not of the Δ*iolT* mutant or Δ*iolG* mutant (Fig. 4A). Thus, *L. pneumophila* appears to utilize inositol in *D. discoideum* and *A. castellanii* amoebae in a similar manner.

To test whether an exogenously added carbohydrate substrate can reach the LCV, we used a green fluorescent glucose analogue, 2-deoxy-2-[(7-nitro-2,1,3-benzoxadiazol-4-yl)-amino]-D-glucose (2-NBDG). *D. discoideum* cells were treated with 2-NBDG 1 h after the infection with *L. pneumophila* strains, and accumulation of the probe in the LCV lumen was monitored by fluorescence microscopy. Indeed, in *D. discoideum* infected with DsRed-producing *L. pneumophila* strain JR32, the Δ*iolT* mutant, or the Δ*iolG* mutant, 2-NBDG localized in a punctate manner inside the amoebae, and the fluorescent glucose analogue accumulated in close proximity to the intracellular bacteria, i.e., in the LCV lumen (Fig. 4B). The quantification of 2-NBDG-positive pathogen vacuoles in intact infected amoebae revealed that approximately 60% of LCVs harboring *L. pneumophila* strain JR32, the Δ*iolT* mutant, or the Δ*iolG* mutant were positive for the fluorescent glucose analogue (Fig. 4C). In contrast, significantly less 2-NBDG accumulated around DsRed-producing mutant bacteria lacking a functional Icm/Dot T4SS (Δ*icmT* mutant) or the alternative sigma factor RpoS (Δ*rpoS* mutant). In *D. discoideum* infected with these mutant strains, only around 30% of the pathogen vacuoles were 2-NBDG positive. The Δ*icmT* mutant and Δ*rpoS* mutant strains are defective for intracellular growth and do not form a replication-permissive LCV but rather localize in bactericidal phagolysosomes.

The findings obtained with intact infected *D. discoideum* were also confirmed by analyzing LCVs in homogenates from amoebae infected with *L. pneumophila* JR32 (Fig. 4D). The infected cells were homogenized after incubation with 2-NBDG, washed thoroughly, and then stained for SidC, an *L. pneumophila* effector protein that specifically localizes to LCV membranes. Using this approach, approximately 60% of the LCVs stained positive for 2-NBDG, similar to what was observed with intact *L. pneumophila*-infected amoebae. As the samples were washed several times in the course of the experiments, the observed fluorescence was retained inside membrane-confined compartments, confirming that 2-NBDG accumulated in the LCV lumen of infected amoebae. Taken together, the fluorescent glucose analogue 2-NBDG accumulates in the replication-permissive LCV but not in a bactericidal compartment. The results suggest that intracellular *L. pneumophila* utilizes carbohydrates (glucose and inositol), which are directly transported from the extracellular milieu to the LCV lumen and not previously metabolized by the host cell. This notion is also in agreement with the finding that the observed intracellular growth stimulation by inositol requires an intact inositol degradation pathway.

***L. pneumophila lpg1653* encodes an inositol transporter.** Since inositol promotes the intracellular growth of *L. pneumophila* and apparently is directly metabolized, we next analyzed whether *L. pneumophila* can take up and utilize inositol. Even though inositol did not have a growth-stimulating effect in complex medium or defined minimal medium (Fig. 2A and B; see also Fig. S1 in the supplemental material), we chose for simplicity reasons to assay inositol transport by extracellular bacteria. To this end, the bacteria were grown to post-exponential-growth phase in AYE medium and incubated with radiolabeled [U-$^{14}C_6$]inositol. The treated bacteria were spun onto cellulose nitrate filter disks, washed, and cell-associated radioactivity on the filters was determined using a liquid scintillation counter.

Indeed, *L. pneumophila* strain JR32 did take up [U-$^{14}C_6$]-inositol, and cell-associated radioactivity reached the maximum after 30 min and remained stable for at least 90 min (Fig. 5A). In contrast, no cell-associated radioactivity was measured for the Δ*iolT* mutant strain. This uptake defect was complemented by expressing *lpg1653* from a plasmid. Thus, *lpg1653* was identified as the inositol transporter gene *iolT*, and the corresponding protein was termed IolT, in reference to the described inositol transporters from *B. subtilis* and *S. enterica* (37, 54). Analogous inositol uptake studies were performed with an *L. pneumophila* Δ*iolG* mutant strain. Similar to the parental strain (but in contrast to the Δ*iolT* mutant), the Δ*iolG* mutant accumulated [U-$^{14}C_6$]inositol within 20 to 30 min, and cell-associated radioactivity remained stable for at least 90 min (Fig. 5B).

To test whether inositol was catabolized and incorporated into cell matter by *L. pneumophila*, bacteria growing exponentially in AYE medium were incubated with [U-$^{14}C_6$]inositol for several hours, and every 2 h, samples were taken and mixed with trichloroacetic acid to precipitate proteins. The samples were then spun onto cellulose nitrate filter disks, and incorporation of radioactivity into the acid-insoluble fraction was measured using a liquid scintillation counter. For the parental strain JR32, radioactivity steadily increased during an 8-h time course, indicating that inositol was indeed used as a precursor for macromolecules, while no radioactivity was detectable in the acid-insoluble fractions of the Δ*iolT* mutant (Fig. 5C) or Δ*iolG* mutant strain (Fig. 5D).

In summary, we identified the *lpg1653* (*iolT*) gene product as the inositol transporter IolT that facilitates inositol uptake by *L. pneumophila*. Consequently, *iolT* is required for incorporation of ^{14}C-label into macromolecules. Contrarily, the *iolG* gene product is dispensable for inositol transport but still essential for inositol metabolism, in agreement with its predicted function as the inositol-2-dehydrogenase.

Expression of P_{iol} is regulated by RpoS and the availability of serine. The predicted and experimentally verified promoter of the *iol* operon, P_{iol}, localizes to the 400-bp region between the genes *lpg1653* and *lpg1654* (Fig. 1). No other promoter is predicted within the *iol* operon. To test the expression of the operon under different conditions, a reporter plasmid was constructed with an unstable GFP variant (ASV) under the control of P_{iol} (pCM007).

The expression of the *iol* operon was assessed in AYE broth by GFP fluorescence of *L. pneumophila* cultures that were diluted to a starting OD_{600} of 0.1. Upon analysis of strain JR32, the expression of P_{iol} started to increase after 6 h, peaked at around 13 h, and

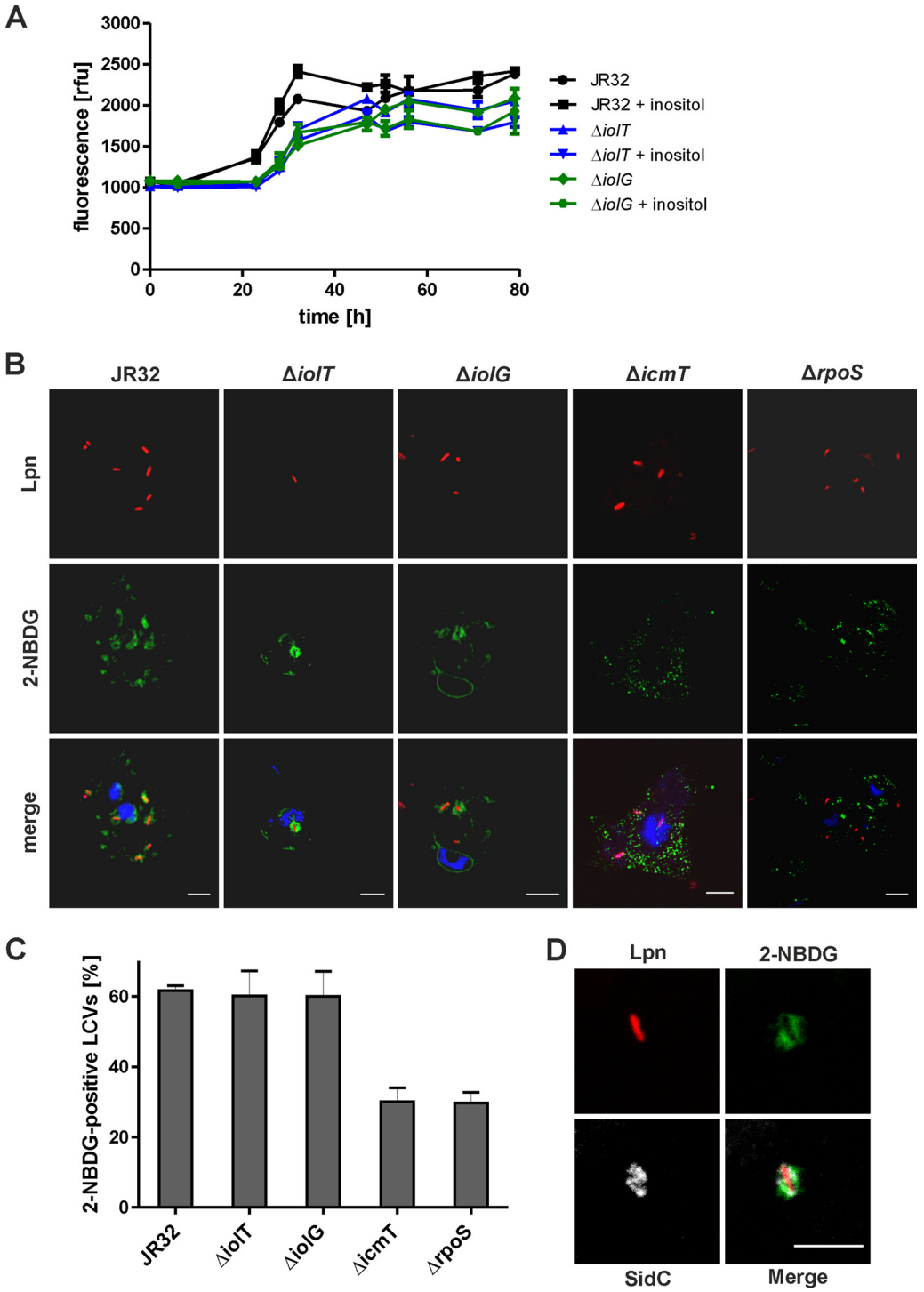

FIG 4 Role of *L. pneumophila* inositol metabolism in *D. discoideum* and accumulation of 2-NBDG in LCVs. (A) *D. discoideum* amoebae were infected (MOI, 10) with *L. pneumophila* JR32, the Δ*iolT* mutant, or the Δ*iolG* mutant harboring plasmid pNT28 (constitutive GFP production). Inositol at 20 mM was added 2 h postinfection, and intracellular replication was determined by fluorescence. The data represent means and SD of triplicates (Student's *t* test; JR32 with or without inositol, $P < 0.05$ at 32 to 47 h; JR32 versus the Δ*iolT* mutant or Δ*iolG* mutant, $P < 0.01$ at 23 to 32 h). (B) *D. discoideum* was infected (MOI, 10) with *L. pneumophila* (Lpn) JR32, Δ*iolT* mutant, Δ*iolG* mutant, Δ*icmT* mutant, or Δ*rpoS* mutant harboring plasmid pSW001 (constitutive DsRed production) for 1 h. The infected amoebae were washed and incubated with 20 μM 2-NBDG for 30 min. Subsequently, the amoebae were washed again and fixed with paraformaldehyde (PFA), stained with DAPI, and subjected to fluorescence microscopy (B and C), or homogenized using a ball homogenizer, fixed with PFA on poly-L-lysine-coated coverslips, and stained for the LCV-bound *L. pneumophila* effector SidC (D). Scale bars = 5 μm. (C) Mean and SD of 2-NBDG-positive LCVs were quantified from three independent experiments counting at least 50 LCVs per experiment.

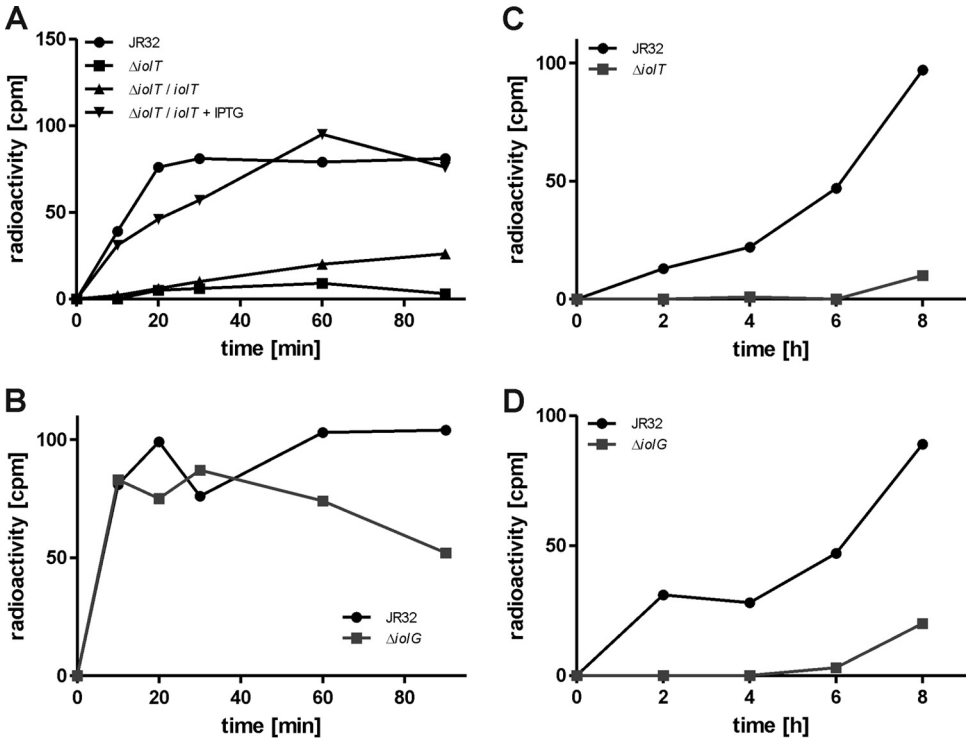

FIG 5 *L. pneumophila lpg1653* encodes an inositol transporter. (A and B) *L. pneumophila* JR32, the Δ*iolT* mutant, or the Δ*iolT* mutant harboring plasmid pCM020 (*iolT* under the control of P_{tac}) (A) or the Δ*iolG* mutant (B) was grown to post-exponential-growth phase, 10 mM inositol mixed with 1% [U-$^{14}C_6$]inositol was added, and the cells were further incubated. After 0, 10, 20, 30, 60, and 90 min, samples were taken, the cells were spun onto cellulose acetate filter disks, and cell-associated radioactivity was measured using a liquid scintillation counter. *L. pneumophila* JR32, the Δ*iolT* mutant (C), or the Δ*iolG* mutant (D) was grown to exponential-growth phase, 10 mM inositol mixed with 1% [U-$^{14}C_6$]inositol was added, and cells were further incubated. After 0, 2, 4, 6, and 8 h, samples were taken and mixed with 50% trichloroacetic acid. Samples were incubated on ice for 1 h, spun onto cellulose nitrate filter disks, and washed, and filter-associated radioactivity was determined using a liquid scintillation counter. The data are from one experiment and representative of the results from three independent experiments.

sharply declined again afterwards in the course of a 24-h growth period (Fig. 6A). Thus, the highest expression levels of P_{iol} were seen in the late-exponential-growth phase of *L. pneumophila*. The addition of 10 mM inositol did not alter *iol* expression, and therefore, the availability of inositol does not seem to autoregulate inositol degradation. Interestingly, however, the addition of 6 mM serine resulted in higher expression levels of P_{iol} and shifted the maximum level from around 13 h to 16 h of growth (Fig. 6A).

Next, we analyzed the role of the *Legionella* quorum-sensing (Lqs) system for the expression of P_{iol}. The Lqs system produces and responds to the small signaling molecule 3-hydroxypentadecane-4-one, LAI-1 (55), and is a component of the stationary-phase regulatory network of *L. pneumophila* (14, 47, 56, 57). To assess whether the Lqs system regulates the *iol* operon, the expression of P_{iol} was assayed in a mutant strain lacking the response regulator LqsR. Compared to the parental strain, no differences were detectable, and again, inositol did not affect P_{iol} expression, while serine enhanced it (Fig. 6B). Virtually identical results were obtained for *L. pneumophila* mutant strains lacking *lqsA*, *lqsS*, *lqsT*, or *lqsS* and *lqsT* (see Fig. S3 in the supplemental material). Therefore, the expression of P_{iol} is not regulated by the Lqs system.

The alternative sigma factor RpoS is a central regulator of intracellular replication and differentiation in *L. pneumophila* (11, 12, 58) and regulates many genes in stationary-growth phase (13, 59). To test whether RpoS controls the expression of the *iol* operon, the P_{iol} reporter construct was assayed in a *L. pneumophila* strain lacking *rpoS*. In the Δ*rpoS* mutant, the expression of *iol* was significantly reduced compared to that in the parental strain, indicating that P_{iol} is indeed regulated by RpoS (Fig. 6C). Inositol did not affect P_{iol} expression in the Δ*rpoS* mutant strain, similarly to what was observed in *L. pneumophila* JR32 or the Δ*lqsR* mutant. Yet, in contrast to these strains, serine also had no effect on P_{iol} expression in the Δ*rpoS* mutant.

Regulation of the *L. pneumophila iol* operon by RpoS was confirmed in experiments measuring the uptake of [U-$^{14}C_6$]inositol at different growth stages (Fig. 6D). At an OD_{600} of 0.5 (early exponential-growth phase), no cell-associated radioactivity was measured for *L. pneumophila* strain JR32 or the Δ*rpoS* mutant, and thus, the strains did not transport or accumulate inositol. However, while for the parental strain increased radioactivity was detectable at OD_{600} of 1.0 (exponential-growth phase), 2.0 (late-exponential-growth phase), and 3.0 (stationary-growth phase), no cell-associated radioactivity was measured for the Δ*rpoS* mutant at any time point (Fig. 6D). In summary, these results show that the alternative sigma factor RpoS regulates the growth-phase- and serine-dependent expression of the *iol* operon and inositol uptake. *L. pneumophila* transports inositol already at the early stages of growth, but the highest levels of transport and P_{iol} expression were observed in the late-exponential/post-exponential-growth phase.

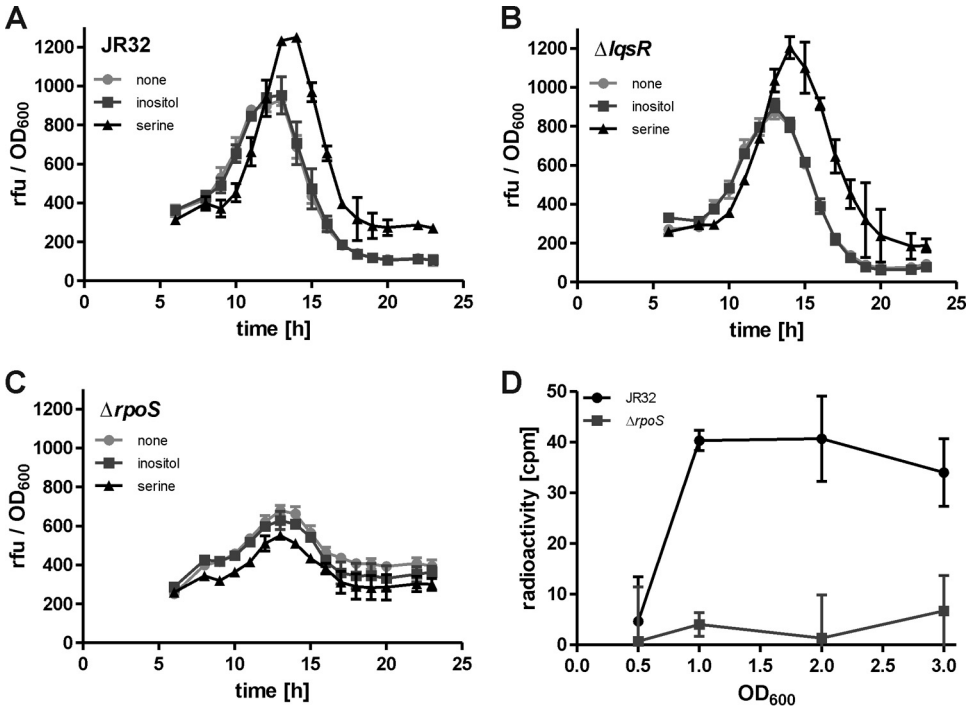

FIG 6 Expression of *iolT* is regulated by RpoS and the availability of serine. Exponentially growing cultures of *L. pneumophila* strain JR32 (A), the Δ*lqsR* mutant (B), or the Δ*rpoS* mutant (C) harboring plasmid pCM007 [unstable GFP(ASV) under the control of P_{iol}] were diluted to a starting OD_{600} of 0.1 in AYE broth. Bacteria were grown at 37°C with 10 mM inositol or 6 mM serine or without the addition of additional nutrients. Optical density at 600 nm and GFP fluorescence were measured every hour for 24 h, and the results were plotted with relative fluorescent units (rfu) as a function of OD_{600} over time. (D) *L. pneumophila* JR32 or the Δ*rpoS* mutant was grown to an OD_{600} of 0.5, 1.0, 2.0, and 3.0. At these points, samples were taken, 10 mM inositol mixed with 1% [U-$^{14}C_6$]inositol was added, and the bacteria were further incubated for 20 min. Cells were spun onto cellulose acetate filter disks and washed, and filter-associated radioactivity was determined in a liquid scintillation counter. The mean and SD of triplicates are shown (Student's *t* test; A and B [serine versus none], >14 h, $P < 0.05$; D, OD_{600}, >1.0, $P < 0.05$). The data are representative of the results from three independent experiments.

DISCUSSION

In this study, we show that *L. pneumophila* metabolizes inositol to promote intracellular growth and virulence. While inositol clearly had an effect on intracellular bacterial growth, the carbohydrate did not stimulate extracellular growth of *L. pneumophila* in several different media used (AYE, CDM, and MDM). AYE is a complex medium containing yeast extract and undefined carbon sources. CDM and MDM do not contain carbohydrates or glycerol; yet, both media contain amino acids in the millimolar range, which likely serve as carbon sources for *L. pneumophila*. Since serine positively affects the expression of the *iol* cluster, catabolite repression due to this amino acid (or perhaps in general) does not seem to account for the observed lack of growth stimulation by inositol in these media.

Inositol metabolism involves the inositol transporter IolT as well as the inositol-2-dehydrogenase IolG. The *L. pneumophila* genes required for the catabolism of inositol are organized in the operon *lpg1653* to *lpg1649*. All genes of the operon show high similarity to corresponding inositol catabolism genes in *B. subtilis* or *S. enterica* (37, 39). However, no gene encoding the malonate-semialdehyde dehydrogenase IolA and the bisphosphate aldolase IolJ are found within the operon or elsewhere in the *L. pneumophila* genome.

In *L. pneumophila*, the methylmalonate-semialdehyde dehydrogenase MmsA (Lpg0129) might substitute for IolA, as predicted by the Kyoto Encyclopedia of Genes and Genomes (KEGG [http://www.genome.jp/kegg/kegg2.html]). Yet, MmsA uses methylmalonate as a substrate producing propionyl-CoA, while IolA uses malonate semialdehyde as a substrate producing acetyl-CoA. Interestingly, the *B. subtilis* enzyme corresponding to MmsA uses methylmalonate semialdehyde or malonate semialdehyde as a substrate for dehydrogenase reactions, producing propionyl-CoA or acetyl-CoA, respectively (60, 61). Since *L. pneumophila* and *B. subtilis* MmsA share 42% identity on the amino acid level, the *Legionella* enzyme might also catalyze the dehydrogenation of methylmalonate semialdehyde as well as malonate semialdehyde.

A substitution for IolJ apparently missing in *L. pneumophila* is more difficult to find. IolJ catalyzes the aldolase reaction with 2-deoxy-5-keto-D-gluconate-6-phosphate as the substrate, yielding dihydroxyacetone phosphate and malonate semialdehyde. *S. enterica* also does not harbor an *iolJ* homologue but can grow on inositol as a sole source of carbon and energy (39), in apparent contrast to *L. pneumophila*. Perhaps, an unidentified *L. pneumophila* aldolase can substitute for IolJ. Alternatively, *L. pneumophila* might employ a novel inositol catabolic pathway, as shown for *Thermotoga maritima* (62). Yet, this is rather unlikely, as all other proteins encoded by the *iol* cluster resemble enzymes that were described in *B. subtilis* and *S. enterica*.

Inositol metabolism in *B. subtilis*, *S. enterica*, or *L. casei* is regulated by IolR (37, 38, 54). In the absence of inositol, IolR binds as a repressor to the operator sequences of inositol transporter (*iolT*) and metabolism genes, and if inositol is available, a catabolic in-

termediate of inositol metabolism acts as a derepressor of IolR (37, 63). *L. pneumophila* does not harbor an *iolR* homologue, and accordingly, the addition of inositol did not affect the expression of *iol*. However, *iol* expression is positively regulated by the amino acid serine. Serine might directly act on regulatory proteins to control gene expression, as shown for gene regulation by arginine (64). Since serine is a major carbon source for *L. pneumophila*, the amino acid might indirectly regulate the expression of *iol* and other genes through a link to the overall metabolic state of the bacteria, which is controlled by the stringent response regulatory cascade and the second messenger guanosine-3′,5′-bispyrophosphate (ppGpp).

The guanosine tetraphosphate (ppGpp) "alarmone" controls the switch between the replicative/nonmotile and the stationary/transmissive forms of *L. pneumophila* in response to limitations of amino acids or other nutrients (65, 66). The signal is synthesized by two enzymes in *L. pneumophila*, RelA and SpoT. RelA is a ribosome-associated enzyme that is activated when uncharged tRNAs accumulate at the ribosome as a consequence of low amino acid levels in the cell (67). SpoT interacts with the acyl-carrier protein (ACP) and is activated by a reduction in the rate of fatty acid biosynthesis or increased levels of short-chain fatty acids (68). The enzyme therefore synthesizes ppGpp by monitoring fatty acid biosynthesis. Furthermore, during exponential growth, SpoT acts as a ppGpp hydrolase, which keeps the concentration of the alarmone low (67). In a previous study, we showed that the metabolism of serine results in a high rate of fatty acid biosynthesis (28), and thus, the SpoT-dependent cellular levels of ppGpp are likely decreased under these conditions.

The alternative sigma factor RpoS is another pivotal regulator of the *iol* operon in *L. pneumophila*. We show here that in a Δ*rpoS* mutant strain, the expression of *iol* is reduced and insensitive to serine. In line with these results, *iolG* is downregulated in *L. pneumophila* lacking *rpoS* upon extracellular growth in water (69). Moreover, RpoS positively regulates carbohydrate metabolism during intracellular multiplication of *L. pneumophila* (13). The alternative sigma factor and the stringent response (SpoT) are linked through a negative-feedback loop: during exponential growth, the ppGpp concentration in the cell is low due to the availability of nutrients and the ppGpp hydrolase activity of SpoT, resulting in the expression of metabolism genes by RpoS (69). When nutrients become limiting and ppGpp concentrations in the cell rise, the stability and activity of RpoS change, and the expression profile switches to virulence and transmission traits (13, 59).

In the stationary-growth phase, RpoS positively regulates a plethora of virulence-related genes, including some that encode Icm/Dot-translocated effector proteins, small regulatory RNAs, and two-component systems (13). The role of RpoS in regulating virulence as well as inositol metabolism is in agreement with the notion that inositol is used as an intracellular carbon source by *L. pneumophila*. Indeed, mutant strains lacking *iolT* or *iolG* had a severe fitness disadvantage compared to the parental strain, and inositol promoted intracellular growth dependent on IolT and IolG in *A. castellanii*, *D. discoideum*, and murine macrophages. Furthermore, the transcriptome of *L. pneumophila* growing in macrophages suggests that inositol is used by the bacteria as a carbon source, since the expression of *iolG* and *iolCB* was upregulated more than 2-fold compared to exponentially growing bacteria (53).

Inositol is likely metabolized directly by intracellular *L. pneumophila* residing in an LCV. This is substantiated by the following findings: (i) inositol (and not a "secondary product") is metabolized, as intracellular growth promotion by the carbohydrate is dependent on *iolT* or *iolG*, (ii) inositol reaches the LCV after phagosome closure and pathogen vacuole formation, since the compound promotes growth when added several hours after infection, (iii) the fluorescent glucose analogue 2-NBDG accumulates in vacuoles harboring strain JR32 but not *icmT* mutant bacteria, and (iv) glycerol and glucose also reach LCVs during intracellular growth of *L. pneumophila* in *A. castellanii* (28). Noteworthy, compared to LCVs, 50% fewer vacuoles harboring *icmT* (or *rpoS*) mutant bacteria accumulate 2-NBDG, indicating that vacuole remodelling by a functional Icm/Dot T4SS is required for carbohydrate transport. We used 2-NBDG as a surrogate sugar substrate, since a fluorescent inositol analog is not available. Hence, this approach might be valid if extracellular carbohydrates reach the LCV lumen via macropinocytotic processes, but not if sugar-specific transmembrane transporters are involved.

2-NBDG has been used to study glucose uptake and metabolism in different organisms and is presumably transported by canonical glucose transporters of the cell (70). Import into LCVs might thus be mediated through host cell transporters acquired by fusion with endosomal or secretory vesicles. Indeed, transport proteins of the solute carrier family of transporters, including amino acid and glucose transporters, have been identified in the proteome of purified LCVs (71), and *L. pneumophila* exploits host cell amino acid transporters for its nutrition (72). Alternatively, 2-NBDG might reach LCVs through endocytic uptake, like macropinocytosis and subsequent membrane fusion processes. *D. discoideum* amoebae take up fluid-phase material via macropinocytosis (73) and presumably also accumulate 2-NBDG through this process. For heterotrophic plant cells, it was shown that 2-NBDG, and therefore likely glucose, inositol, or other substrates, can also be taken up by endocytic processes and accumulate in vesicles and vacuoles (74). Endocytic events might also account for the (less-efficient) accumulation of 2-NBDG in vacuoles containing *L. pneumophila* lacking a functional Icm/Dot T4SS.

Icm/Dot-translocated effector proteins might also play a role in the acquisition of inositol by *L. pneumophila* during intracellular growth. LppA is an Icm/Dot T4SS-translocated cysteine phytase, which seems to detoxify bacteriostatic phytate within infected amoebae producing the chelator in millimolar quantities (36). The bacterial phytase LppA might promote intracellular replication not only by increasing micronutrient (iron) availability to *L. pneumophila* but also by production from phytate inositol phosphates or inositol, which can be used by the bacteria. Inositol transporters of the solute carrier family 5 and family 2 facilitate uptake of inositol in mammalian cells (75) and, perhaps, also into the LCV. The bacterial inositol transporter IolT could then import inositol from the LCV lumen into the bacterial cell, where it is metabolized.

Taken together, available evidence indicates that inositol is metabolized through the *iol* gene products by *L. pneumophila* during intracellular growth. Inositol is also taken up and presumably utilized under extracellular conditions. These results extend the proven metabolic capacities of *L. pneumophila* by another carbohydrate carbon source. Further investigations on inositol metabolism by *L. pneumophila* will elucidate its detailed mechanisms and will clarify if and how inositol contributes to the bipartite

metabolism of *L. pneumophila* (28). These studies will shed new light on the nutrition of *Legionella* spp., particularly inside host cells, and its effects on virulence.

ACKNOWLEDGMENTS

We would like to thank for generous funding the Swiss National Science Foundation (SNF) (grant 31003A_153200), the German Research Foundation (DFG) (grants SPP1316 and SPP1617), and the Bundesministerium für Bildung und Forschung (BMBF) for funding provided through the program Infect-ERA in the context of the EUGENPATH network (grant 031A410A).

FUNDING INFORMATION

This work, including the efforts of Hubert Hilbi, was funded by Deutsche Forschungsgemeinschaft (DFG) (SPP1316 and SPP1617). This work, including the efforts of Hubert Hilbi, was funded by Schweizerischer Nationalfonds zur Förderung der Wissenschaftlichen Forschung (SNF) (31003A_153200). This work, including the efforts of Hubert Hilbi, was funded by Bundesministerium für Bildung und Forschung (BMBF) (Infect-ERA project EUGENPATH [031A410A]).

The funders had no role in the study design, data collection and interpretation, or the decision to submit the work for publication.

REFERENCES

1. **Abdel-Nour M, Duncan C, Low DE, Guyard C.** 2013. Biofilms: the stronghold of *Legionella pneumophila*. Int J Mol Sci **14:**21660–21675. http://dx.doi.org/10.3390/ijms141121660.
2. **Hilbi H, Hoffmann C, Harrison CF.** 2011. *Legionella* spp. outdoors: colonization, communication and persistence. Environ Microbiol Rep **3:**286–296. http://dx.doi.org/10.1111/j.1758-2229.2011.00247.x.
3. **Mampel J, Spirig T, Weber SS, Haagensen JAJ, Molin S, Hilbi H.** 2006. Planktonic replication is essential for biofilm formation by *Legionella pneumophila* in a complex medium under static and dynamic flow conditions. Appl Environ Microbiol **72:**2885–2895. http://dx.doi.org/10.1128/AEM.72.4.2885-2895.2006.
4. **Fields BS.** 1996. The molecular ecology of legionellae. Trends Microbiol **4:**286–290. http://dx.doi.org/10.1016/0966-842X(96)10041-X.
5. **Hoffmann C, Harrison CF, Hilbi H.** 2014. The natural alternative: protozoa as cellular models for *Legionella* infection. Cell Microbiol **16:**15–26. http://dx.doi.org/10.1111/cmi.12235.
6. **Newton HJ, Ang DK, van Driel IR, Hartland EL.** 2010. Molecular pathogenesis of infections caused by *Legionella pneumophila*. Clin Microbiol Rev **23:**274–298. http://dx.doi.org/10.1128/CMR.00052-09.
7. **Isberg RR, O'Connor TJ, Heidtman M.** 2009. The *Legionella pneumophila* replication vacuole: making a cosy niche inside host cells. Nat Rev Microbiol **7:**13–24. http://dx.doi.org/10.1038/nrmicro1967.
8. **Hubber A, Roy CR.** 2010. Modulation of host cell function by *Legionella pneumophila* type IV effectors. Annu Rev Cell Dev Biol **26:**261–283. http://dx.doi.org/10.1146/annurev-cellbio-100109-104034.
9. **Haneburger I, Hilbi H.** 2013. Phosphoinositide lipids and the *Legionella* pathogen vacuole. Curr Top Microbiol Immunol **376:**155–173.
10. **Finsel I, Hilbi H.** 2015. Formation of a pathogen vacuole according to *Legionella pneumophila*: how to kill one bird with many stones. Cell Microbiol **17:**935–950. http://dx.doi.org/10.1111/cmi.12450.
11. **Bachman MA, Swanson MS.** 2001. RpoS co-operates with other factors to induce *Legionella pneumophila* virulence in the stationary phase. Mol Microbiol **40:**1201–1214. http://dx.doi.org/10.1046/j.1365-2958.2001.02465.x.
12. **Hales LM, Shuman HA.** 1999. The *Legionella pneumophila rpoS* gene is required for growth within *Acanthamoeba castellanii*. J Bacteriol **181:**4879–4889.
13. **Hovel-Miner G, Pampou S, Faucher SP, Clarke M, Morozova I, Morozov P, Russo JJ, Shuman HA, Kalachikov S.** 2009. SigmaS controls multiple pathways associated with intracellular multiplication of *Legionella pneumophila*. J Bacteriol **191:**2461–2473. http://dx.doi.org/10.1128/JB.01578-08.
14. **Tiaden A, Spirig T, Weber SS, Brüggemann H, Bosshard R, Buchrieser C, Hilbi H.** 2007. The *Legionella pneumophila* response regulator LqsR promotes host cell interactions as an element of the virulence regulatory network controlled by RpoS and LetA. Cell Microbiol **9:**2903–2920. http://dx.doi.org/10.1111/j.1462-5822.2007.01005.x.
15. **Tiaden A, Spirig T, Hilbi H.** 2010. Bacterial gene regulation by α-hydroxyketone signaling. Trends Microbiol **18:**288–297. http://dx.doi.org/10.1016/j.tim.2010.03.004.
16. **Abu Kwaik Y, Bumann D.** 2013. Microbial quest for food *in vivo*: 'nutritional virulence' as an emerging paradigm. Cell Microbiol **15:**882–890. http://dx.doi.org/10.1111/cmi.12138.
17. **Manske C, Hilbi H.** 2014. Metabolism of the vacuolar pathogen *Legionella* and implications for virulence. Front Cell Infect Microbiol **4:**125.
18. **Pine L, George JR, Reeves MW, Harrell WK.** 1979. Development of a chemically defined liquid medium for growth of *Legionella pneumophila*. J Clin Microbiol **9:**615–626.
19. **Ristroph JD, Hedlund KW, Gowda S.** 1981. Chemically defined medium for *Legionella pneumophila* growth. J Clin Microbiol **13:**115–119.
20. **Tesh MJ, Miller RD.** 1981. Amino acid requirements for *Legionella pneumophila* growth. J Clin Microbiol **13:**865–869.
21. **Tesh MJ, Morse SA, Miller RD.** 1983. Intermediary metabolism in *Legionella pneumophila*: utilization of amino acids and other compounds as energy sources. J Bacteriol **154:**1104–1109.
22. **Eylert E, Herrmann V, Jules M, Gillmaier N, Lautner M, Buchrieser C, Eisenreich W, Heuner K.** 2010. Isotopologue profiling of *Legionella pneumophila*: role of serine and glucose as carbon substrates. J Biol Chem **285:**22232–22243. http://dx.doi.org/10.1074/jbc.M110.128678.
23. **Chien M, Morozova I, Shi S, Sheng H, Chen J, Gomez SM, Asamani G, Hill K, Nuara J, Feder M, Rineer J, Greenberg JJ, Steshenko V, Park SH, Zhao B, Teplitskaya E, Edwards JR, Pampou S, Georghiou A, Chou IC, Iannuccilli W, Ulz ME, Kim DH, Geringer-Sameth A, Goldsberry C, Morozov P, Fischer SG, Segal G, Qu X, Rzhetsky A, Zhang P, Cayanis E, De Jong PJ, Ju J, Kalachikov S, Shuman HA, Russo JJ.** 2004. The genomic sequence of the accidental pathogen *Legionella pneumophila*. Science **305:**1966–1968. http://dx.doi.org/10.1126/science.1099776.
24. **Cazalet C, Rusniok C, Brüggemann H, Zidane N, Magnier A, Ma L, Tichit M, Jarraud S, Bouchier C, Vandenesch F, Kunst F, Etienne J, Glaser P, Buchrieser C.** 2004. Evidence in the *Legionella pneumophila* genome for exploitation of host cell functions and high genome plasticity. Nat Genet **36:**1165–1173. http://dx.doi.org/10.1038/ng1447.
25. **D'Auria G, Jimenez-Hernandez N, Peris-Bondia F, Moya A, Latorre A.** 2010. *Legionella pneumophila* pangenome reveals strain-specific virulence factors. BMC Genomics **11:**181. http://dx.doi.org/10.1186/1471-2164-11-181.
26. **Keen MG, Hoffman PS.** 1984. Metabolic pathways and nitrogen metabolism in *Legionella pneumophila*. Curr Microbiol **11:**81–88. http://dx.doi.org/10.1007/BF01567708.
27. **Harada E, Iida K, Shiota S, Nakayama H, Yoshida S.** 2010. Glucose metabolism in *Legionella pneumophila*: dependence on the Entner-Doudoroff pathway and connection with intracellular bacterial growth. J Bacteriol **192:**2892–2899. http://dx.doi.org/10.1128/JB.01535-09.
28. **Häuslein I, Manske C, Goebel W, Eisenreich W, Hilbi H.** 2016. Pathway analysis using ^{13}C-glycerol and other carbon tracers reveals a bipartite metabolism of *Legionella pneumophila*. Mol Microbiol **100:**229–246. http://dx.doi.org/10.1111/mmi.13313.
29. **Grubmüller S, Schauer K, Goebel W, Fuchs TM, Eisenreich W.** 2014. Analysis of carbon substrates used by *Listeria monocytogenes* during growth in J774A.1 macrophages suggests a bipartite intracellular metabolism. Front Cell Infect Microbiol **4:**156.
30. **de Carvalho LP, Fischer SM, Marrero J, Nathan C, Ehrt S, Rhee KY.** 2010. Metabolomics of *Mycobacterium tuberculosis* reveals compartmentalized co-catabolism of carbon substrates. Chem Biol **17:**1122–1131. http://dx.doi.org/10.1016/j.chembiol.2010.08.009.
31. **Beste DJ, Noh K, Niedenfuhr S, Mendum TA, Hawkins ND, Ward JL, Beale MH, Wiechert W, McFadden J.** 2013. ^{13}C-flux spectral analysis of host-pathogen metabolism reveals a mixed diet for intracellular *Mycobacterium tuberculosis*. Chem Biol **20:**1012–1021. http://dx.doi.org/10.1016/j.chembiol.2013.06.012.
32. **Turner BL, Paphazy MJ, Haygarth PM, McKelvie ID.** 2002. Inositol phosphates in the environment. Philos Trans R Soc Lond B Biol Sci **357:**449–469. http://dx.doi.org/10.1098/rstb.2001.0837.
33. **Lim BL, Yeung P, Cheng C, Hill JE.** 2007. Distribution and diversity of phytate-mineralizing bacteria. ISME J **1:**321–330.
34. **Rao DE, Rao KV, Reddy TP, Reddy VD.** 2009. Molecular characterization, physicochemical properties, known and potential applications of

phytases: an overview. Crit Rev Biotechnol **29:**182–198. http://dx.doi.org/10.1080/07388550902919571.
35. **Urbano G, Lopez-Jurado M, Aranda P, Vidal-Valverde C, Tenorio E, Porres J.** 2000. The role of phytic acid in legumes: antinutrient or beneficial function? J Physiol Biochem **56:**283–294. http://dx.doi.org/10.1007/BF03179796.
36. **Weber S, Stirnimann CU, Wieser M, Frey D, Meier R, Engelhardt S, Li X, Capitani G, Kammerer RA, Hilbi H.** 2014. A type IV translocated *Legionella* cysteine phytase counteracts intracellular growth restriction by phytate. J Biol Chem **289:**34175–34188. http://dx.doi.org/10.1074/jbc.M114.592568.
37. **Yoshida K, Yamaguchi M, Morinaga T, Kinehara M, Ikeuchi M, Ashida H, Fujita Y.** 2008. *myo*-Inositol catabolism in *Bacillus subtilis*. J Biol Chem **283:**10415–10424. http://dx.doi.org/10.1074/jbc.M708043200.
38. **Yebra MJ, Zuniga M, Beaufils S, Perez-Martinez G, Deutscher J, Monedero V.** 2007. Identification of a gene cluster enabling *Lactobacillus casei* BL23 to utilize *myo*-inositol. Appl Environ Microbiol **73:**3850–3858. http://dx.doi.org/10.1128/AEM.00243-07.
39. **Kröger C, Fuchs TM.** 2009. Characterization of the *myo*-inositol utilization island of *Salmonella enterica* serovar Typhimurium. J Bacteriol **191:**545–554. http://dx.doi.org/10.1128/JB.01253-08.
40. **Kohler PR, Zheng JY, Schoffers E, Rossbach S.** 2010. Inositol catabolism, a key pathway in *Sinorhizobium meliloti* for competitive host nodulation. Appl Environ Microbiol **76:**7972–7980. http://dx.doi.org/10.1128/AEM.01972-10.
41. **Yoshida K, Yamamoto Y, Omae K, Yamamoto M, Fujita Y.** 2002. Identification of two *myo*-inositol transporter genes of *Bacillus subtilis*. J Bacteriol **184:**983–991. http://dx.doi.org/10.1128/jb.184.4.983-991.2002.
42. **Yoshida KI, Shibayama T, Aoyama D, Fujita Y.** 1999. Interaction of a repressor and its binding sites for regulation of the *Bacillus subtilis iol* divergon. J Mol Biol **285:**917–929. http://dx.doi.org/10.1006/jmbi.1998.2398.
43. **Zhou K, Takegawa K, Emr SD, Firtel RA.** 1995. A phosphatidylinositol (PI) kinase gene family in *Dictyostelium discoideum*: biological roles of putative mammalian p110 and yeast Vps34p PI3-kinase homologs during growth and development. Mol Cell Biol **15:**5645–5656. http://dx.doi.org/10.1128/MCB.15.10.5645.
44. **Andersen JB, Sternberg C, Poulsen LK, Bjorn SP, Givskov M, Molin S.** 1998. New unstable variants of green fluorescent protein for studies of transient gene expression in bacteria. Appl Environ Microbiol **64:**2240–2246.
45. **Wiater LA, Sadosky AB, Shuman HA.** 1994. Mutagenesis of *Legionella pneumophila* using Tn*903*dll*lacZ*: identification of a growth-phase-regulated pigmentation gene. Mol Microbiol **11:**641–653. http://dx.doi.org/10.1111/j.1365-2958.1994.tb00343.x.
46. **Harrison CF, Kicka S, Trofimov V, Berschl K, Ouertatani-Sakouhi H, Ackermann N, Hedberg C, Cosson P, Soldati T, Hilbi H.** 2013. Exploring anti-bacterial compounds against intracellular *Legionella*. PLoS One **8:**e74813. http://dx.doi.org/10.1371/journal.pone.0074813.
47. **Kessler A, Schell U, Sahr T, Tiaden A, Harrison C, Buchrieser C, Hilbi H.** 2013. The *Legionella pneumophila* orphan sensor kinase LqsT regulates competence and pathogen-host interactions as a component of the LAI-1 circuit. Environ Microbiol **15:**646–662. http://dx.doi.org/10.1111/j.1462-2920.2012.02889.x.
48. **Weber SS, Ragaz C, Reus K, Nyfeler Y, Hilbi H.** 2006. *Legionella pneumophila* exploits PI(4)*P* to anchor secreted effector proteins to the replicative vacuole. PLoS Pathog **2:**e46. http://dx.doi.org/10.1371/journal.ppat.0020046.
49. **Mao F, Dam P, Chou J, Olman V, Xu Y.** 2009. DOOR: a database for prokaryotic operons. Nucleic Acids Res **37:**D459–D463. http://dx.doi.org/10.1093/nar/gkn757.
50. **Sahr T, Rusniok C, Dervins-Ravault D, Sismeiro O, Coppee JY, Buchrieser C.** 2012. Deep sequencing defines the transcriptional map of *L. pneumophila* and identifies growth phase-dependent regulated ncRNAs implicated in virulence. RNA Biol **9:**503–519. http://dx.doi.org/10.4161/rna.20270.
51. **Cazalet C, Gomez-Valero L, Rusniok C, Lomma M, Dervins-Ravault D, Newton HJ, Sansom FM, Jarraud S, Zidane N, Ma L, Bouchier C, Etienne J, Hartland EL, Buchrieser C.** 2010. Analysis of the *Legionella longbeachae* genome and transcriptome uncovers unique strategies to cause Legionnaires' disease. PLoS Genet **6:**e1000851. http://dx.doi.org/10.1371/journal.pgen.1000851.
52. **Kozak NA, Buss M, Lucas CE, Frace M, Govil D, Travis T, Olsen-Rasmussen M, Benson RF, Fields BS.** 2010. Virulence factors encoded by *Legionella longbeachae* identified on the basis of the genome sequence analysis of clinical isolate D-4968. J Bacteriol **192:**1030–1044. http://dx.doi.org/10.1128/JB.01272-09.
53. **Faucher SP, Mueller CA, Shuman HA.** 2011. *Legionella pneumophila* transcriptome during intracellular multiplication in human macrophages. Front Microbiol **2:**60.
54. **Kröger C, Stolz J, Fuchs TM.** 2010. *myo*-Inositol transport by *Salmonella enterica* serovar Typhimurium. Microbiology **156:**128–138. http://dx.doi.org/10.1099/mic.0.032250-0.
55. **Spirig T, Tiaden A, Kiefer P, Buchrieser C, Vorholt JA, Hilbi H.** 2008. The *Legionella* autoinducer synthase LqsA produces an α-hydroxyketone signaling molecule. J Biol Chem **283:**18113–18123. http://dx.doi.org/10.1074/jbc.M801929200.
56. **Tiaden A, Spirig T, Sahr T, Wälti MA, Boucke K, Buchrieser C, Hilbi H.** 2010. The autoinducer synthase LqsA and putative sensor kinase LqsS regulate phagocyte interactions, extracellular filaments and a genomic island of *Legionella pneumophila*. Environ Microbiol **12:**1243–1259. http://dx.doi.org/10.1111/j.1462-2920.2010.02167.x.
57. **Tiaden A, Hilbi H.** 2012. α-Hydroxyketone synthesis and sensing by *Legionella* and *Vibrio*. Sensors (Basel) **12:**2899–2919. http://dx.doi.org/10.3390/s120302899.
58. **Rasis M, Segal G.** 2009. The LetA-RsmYZ-CsrA regulatory cascade, together with RpoS and PmrA, post-transcriptionally regulates stationary phase activation of *Legionella pneumophila* Icm/Dot effectors. Mol Microbiol **72:**995–1010. http://dx.doi.org/10.1111/j.1365-2958.2009.06705.x.
59. **Zusman T, Gal-Mor O, Segal G.** 2002. Characterization of a *Legionella pneumophila relA* insertion mutant and roles of RelA and RpoS in virulence gene expression. J Bacteriol **184:**67–75. http://dx.doi.org/10.1128/JB.184.1.67-75.2002.
60. **Stines-Chaumeil C, Talfournier F, Branlant G.** 2006. Mechanistic characterization of the MSDH (methylmalonate semialdehyde dehydrogenase) from *Bacillus subtilis*. Biochem J **395:**107–115. http://dx.doi.org/10.1042/BJ20051525.
61. **Talfournier F, Stines-Chaumeil C, Branlant G.** 2011. Methylmalonate-semialdehyde dehydrogenase from *Bacillus subtilis*: substrate specificity and coenzyme A binding. J Biol Chem **286:**21971–21981. http://dx.doi.org/10.1074/jbc.M110.213280.
62. **Rodionova IA, Leyn SA, Burkart MD, Boucher N, Noll KM, Osterman AL, Rodionov DA.** 2013. Novel inositol catabolic pathway in *Thermotoga maritima*. Environ Microbiol **15:**2254–2266. http://dx.doi.org/10.1111/1462-2920.12096.
63. **Yoshida KI, Aoyama D, Ishio I, Shibayama T, Fujita Y.** 1997. Organization and transcription of the *myo*-inositol operon, *iol*, of *Bacillus subtilis*. J Bacteriol **179:**4591–4598.
64. **Hovel-Miner G, Faucher SP, Charpentier X, Shuman HA.** 2010. ArgR-regulated genes are derepressed in the *Legionella*-containing vacuole. J Bacteriol **192:**4504–4516. http://dx.doi.org/10.1128/JB.00465-10.
65. **Hammer BK, Swanson MS.** 1999. Co-ordination of *Legionella pneumophila* virulence with entry into stationary phase by ppGpp. Mol Microbiol **33:**721–731. http://dx.doi.org/10.1046/j.1365-2958.1999.01519.x.
66. **Dalebroux ZD, Yagi BF, Sahr T, Buchrieser C, Swanson MS.** 2010. Distinct roles of ppGpp and DksA in *Legionella pneumophila* differentiation. Mol Microbiol **76:**200–219. http://dx.doi.org/10.1111/j.1365-2958.2010.07094.x.
67. **Dalebroux ZD, Edwards RL, Swanson MS.** 2009. SpoT governs *Legionella pneumophila* differentiation in host macrophages. Mol Microbiol **71:**640–658. http://dx.doi.org/10.1111/j.1365-2958.2008.06555.x.
68. **Edwards RL, Dalebroux ZD, Swanson MS.** 2009. *Legionella pneumophila* couples fatty acid flux to microbial differentiation and virulence. Mol Microbiol **71:**1190–1204. http://dx.doi.org/10.1111/j.1365-2958.2008.06593.x.
69. **Trigui H, Dudyk P, Oh J, Hong JI, Faucher SP.** 2015. A regulatory feedback loop between RpoS and SpoT supports the survival of *Legionella pneumophila* in water. Appl Environ Microbiol **81:**918–928. http://dx.doi.org/10.1128/AEM.03132-14.
70. **Yamada K, Nakata M, Horimoto N, Saito M, Matsuoka H, Inagaki N.** 2000. Measurement of glucose uptake and intracellular calcium concentration in single, living pancreatic beta-cells. J Biol Chem **275:**22278–22283. http://dx.doi.org/10.1074/jbc.M908048199.
71. **Hoffmann C, Finsel I, Otto A, Pfaffinger G, Rothmeier E, Hecker M, Becher D, Hilbi H.** 2014. Functional analysis of novel Rab GTPases

identified in the proteome of purified *Legionella*-containing vacuoles from macrophages. Cell Microbiol **16:**1034–1052.
72. **Wieland H, Ullrich S, Lang F, Neumeister B.** 2005. Intracellular multiplication of *Legionella pneumophila* depends on host cell amino acid transporter SLC1A5. Mol Microbiol **55:**1528–1537. http://dx.doi.org/10.1111/j.1365-2958.2005.04490.x.
73. **Hacker U, Albrecht R, Maniak M.** 1997. Fluid-phase uptake by macropinocytosis in *Dictyostelium*. J Cell Sci **110:**105–112.
74. **Etxeberria E, Gonzalez P, Tomlinson P, Pozueta-Romero J.** 2005. Existence of two parallel mechanisms for glucose uptake in heterotrophic plant cells. J Exp Bot **56:**1905–1912. http://dx.doi.org/10.1093/jxb/eri185.
75. **Klaus F, Palmada M, Lindner R, Laufer J, Jeyaraj S, Lang F, Boehmer C.** 2008. Up-regulation of hypertonicity-activated *myo*-inositol transporter SMIT1 by the cell volume-sensitive protein kinase SGK1. J Physiol **586:**1539–1547. http://dx.doi.org/10.1113/jphysiol.2007.146191.
76. **Sadosky AB, Wiater LA, Shuman HA.** 1993. Identification of *Legionella pneumophila* genes required for growth within and killing of human macrophages. Infect Immun **61:**5361–5373.
77. **Segal G, Shuman HA.** 1998. Intracellular multiplication and human macrophage killing by *Legionella pneumophila* are inhibited by conjugal components of IncQ plasmid RSF1010. Mol Microbiol **30:**197–208. http://dx.doi.org/10.1046/j.1365-2958.1998.01054.x.
78. **Andersen JB, Heydorn A, Hentzer M, Eberl L, Geisenberger O, Christensen BB, Molin S, Givskov M.** 2001. *gfp*-based *N*-acyl homoserine-lactone sensor systems for detection of bacterial communication. Appl Environ Microbiol **67:**575–585. http://dx.doi.org/10.1128/AEM.67.2.575-585.2001.